Consequences of Nonlytic Membrane Perturbation to the Translocation of the Cell Penetrating Peptide Pep-1 in Lipidic Vesicles†

Sónia Troeira Henriques and Miguel Augusto Rico Botas Castanho*

Centro de Química e Bioquímica, Faculdade de Ciências da Universidade de Lisboa, Ed. C8, Campo Grande, 1749-016 Lisboa, Portugal

Received December 29, 2003; Revised Manuscript Received April 27, 2004

ABSTRACT: The action of the cell penetrating pep-1 at the molecular level is not clearly understood. The ability of the peptide to induce (1) vesicle aggregation, (2) lipidic fusion, (3) anionic lipid segregation, (4) pore or other lytic structure formation, (5) asymmetric lipidic flip-flop, and (6) peptide translocation across the bilayers in large unilamellar vesicles was studied using photophysical methodologies mainly related to fluorescence spectroscopy. Neflometry and turbidimetry techniques show that clustering of vesicles occurs in the presence of the peptide in a concentration- and anionic lipid content-dependent manner. Results from Forstër resonance energy transfer-based methodologies prove lipidic fusion and anionic lipid segregation, but no evidence for pores or other lytic structures was found. Asymmetric lipid flip-flop was not detected either. A specific method related to the quenching of the rhodamine-labeled lipids by pep-1 was developed to study the eventual translocation of the peptide. Translocation does not occur in symmetrical neutral and negatively charged vesicles, except when a valinomycin-induced transmembrane potential exists. Our work strongly suggests that the main driving force for peptide translocation is charge asymmetry between the outer and inner leaflet of biological membranes and reveals that pep-1 is able to perturb membranes without being cytotoxic. This nonlytic perturbation is probably mandatory for translocation to occur.

The molecular ability to cross the biomembrane barrier and introduce material into cells is a recent matter of interest in research. So far, gene delivery technologies are most used, but these kinds of delivery systems have some drawbacks, such as low efficiency, poor specificity, poor bioavailability, and toxicity (*1*). Introduction of proteins directly into a cell is a better alternative because the posttranslation modification is critical for the biological function of the protein (*2*). Nevertheless traditional methods to introduce proteins have low efficiency; the transduced protein often enters the endocytic pathway and traffics to the lysosome where it will be degraded and inactivated (*2*). New strategies for protein transduction have been developed that use peptide carriers designated as protein transduction domains (PTDs)[1] (*1*−*7*). These "vectors" are basic sequences capable of translocating across the plasmatic membranes in a manner independent of receptors or the endosomal pathway, carrying proteins covalently linked (*1*−*7*).

Pep-1, a synthetic peptide carrier capable of introducing active proteins into cells, has advantages over "genetic therapy" because phenotype can be altered in less than 2 h (*3*, *8*, *9*), as well as over other PTDs since the interaction with proteins is independent of covalent links; the complex pep-1/protein is promoted by hydrophobic forces (*3*, *8*, *10*). The pep-1 has 21 amino acid residues (KETWWETWWTEWSQPKKKRKV), which can be divided into three different domains: a "so-called" hydrophobic one, rich in tryptophans (KETWWETWWTEW), a hydrophilic domain with basic residues (KKKRKV), and a spacer between them (SQP) (*3*, *8*). The hydrophobic sequence is responsible for the hydrophobic interactions with proteins (*3*, *8*) and for the intrinsic fluorescence of the peptide. The hydrophilic domain improves intracellular distribution and the solubility of peptide (*3*, *8*). The spacer sequence is a link between the other two domains (*3*, *8*). Peptide is acetylated on the N terminus and has a cysteamine group on the C terminus (*8*); at physiological pH (7.4), the peptide has a global charge of +3.

Like others PTDs, pep-1 translocates along biological membranes in a manner independent of the endosomal pathway (*8*), which suggests a physical process dictated by the lipid bilayer. Pep-1 has high affinity for lipid bilayers, and the presence of negative charges in the vesicles enhances the partition to lipid bilayers, showing a strong electrostatic interaction (*11*).

In the present paper, our aim is to present functional abilities of the peptide (vesicle aggregation, dissociation, and

† This work was supported by Fundação para a Ciência e Tecnologia (Portugal).

* To whom correspondence should be addressed. Tel.: +351217500931. Fax: +351217500088. E-mail: castanho@fc.ul.pt.

[1] Abbreviations: PTDs, protein transduction domains; HEPES, 2-(4-(2-hydroxyethyl)-1-piperazinyl)ethanesulfonic acid; POPC, 1-palmitoyl-2-oleoyl-*sn*-glycero-3-phosphocholine; POPG, 1-palmitoyl-2-oleoyl-*sn*-glycero-3-(phospho-*rac*-(1-glycerol)); DPPC, 1,2-dipalmitoyl-*sn*-glycero-3-phosphocholine; DPPS, 1,2-dipalmitoyl-*sn*-glycero-3-(phospho-L-serine); C6-NBD-PC, 1-myristoyl-2-[6-[(7-nitro-2−1,3-benzoxadiazol-4-yl)amino]caproil]-*sn*-glycero-3-phosphocholine; C6-NBD-PG, 1-myristoyl-2-[6-[(7-nitro-2−1,3-benzoxadiazol-4-yl)amino]caproil]-*sn*-glycero-3-phosphoglycerol; N-NBD-PE, 1,2-dipalmitoyl-*sn*-glycero-3-phosphoethalonamine-*N*-(7-nitro-2-1,3-benzoxadiazol-4-yl); N-Rh-PE, 1,2-dipalmitoyl-*sn*-glycero-3-phosphoethalonamine-*N*-(lissamine rhodamine B sulfonyl); Rh B, rhodamine B; TX-100, Triton X-100; LUVs, large unilamellar vesicles; MLVs, multilamellar vesicles; FRET, Forstër resonance energy transfer; OD, optical density.

10.1021/bi036325k CCC: $27.50
Published on Web 07/07/2004

fusion, pore formation in the lipidic bilayer, induction of phospholipid flip-flop, segregation of anionic phospholipid, and the ability to translocate) and to propose a molecular model of action.

EXPERIMENTAL PROCEDURES

Reagents and Apparatus. Chariot, the commercial name of pep-1, was obtained from Active Motif (Rixensart, Belgium) with purity >95%; 2-(4-(2-Hydroxyethyl)-1-piperazinyl)ethanesulfonic acid (HEPES), sodium chloride, and chloroform (spectroscopic grade) were from Merk (Darmstadt, Germany); 1-palmitoyl-2-oleoyl-*sn*-glycero-3-phosphocholine (POPC), 1-palmitoyl-2-oleoyl-*sn*-glycero-3-(phospho-*rac*-(1-glycerol)) (POPG), 1,2-dipalmitoyl-*sn*-glycero-3-phosphocholine (DPPC), 1,2-dipalmitoyl-*sn*-glycero-3-(phospho-L-serine) (DPPS), 1-myristoyl-2-[6-[(7-nitro-2-1,3-benzoxadiazol-4-yl)amino]caproil]-*sn*-glycero-3-phosphocholine (C6-NBD-PC), 1-myristoyl-2-[6-[(7-nitrro-2-1,3-benzoxadiazol-4-yl)amino]caproil]-*sn*-glycero-3-phosphoglycerol (C6-NBD-PG), 1,2-dipalmitoyl-*sn*-glycero-3-phosphoethalonamine-*N*-(7-nitro-2-1,3-benzoxadiazol-4-yl) (N-NBD-PE), and 1,2-dipalmitoyl-*sn*-glycero-3-phosphoethalonamine-*N*-(lissamine rhodamine B sulfonyl) (N-Rh-PE) were from Avanti Polar-Lipids (Alabaster, Alabama); Triton X-100 (TX-100), rhodamine B (Rh B), and valinomycin were from Sigma (St. Louis, Missouri); cobalt(II) chloride hexahydrate ($CoCl_2 \cdot 6H_2O$) was from Acrós organics (Geel, Belgium), and tris-(2-cyanoethyl)phosphine (phosphine) was from molecular probes (Eugene, Oregon).

The assays were performed at room temperature in a UV−vis spectrophometer, Jasco V-530, in a spectrofluorometer, SLM Aminco 8100 (equipped with a 450 W Xe lamp, Glan−Thompson polarizers, and double monochromators), and in a fluorescence microscope, Olympus BX41 (using band-pass filters). The microscopy results were recorded in a digital camera, Olympus camedia 4040 zoom. Solutions were prepared in 10 mM HEPES buffer, pH 7.4, containing 150 mM NaCl (the so-called physiologic ionic strength). Osmolalities were measured in a freezing-point depression osmometer (Osmometer Automatic; Knauer, Berlin, Germany).

Preparation of Lipid Vesicles. Large unilamellar vesicles (LUVs) are a good model of biological membranes having no significant curvature effects (typical 100 nm diameter) (*12*). LUVs were prepared by the extrusion method described elsewhere (*13*). To obtain multilamellar vesicles (MLVs), the extrusion step was not performed. To study the effect of transmembrane potential in translocation, LUVs were prepared in HEPES buffer with 150 mM KCl or with 150 mM NaCl and passed through a 10 mL Econo-Pac 10DG column (Bio-Gel P-6DG gel with 6 kDa molecular weight exclusion) packed in buffer containing 150 mM NaCl or 150 mM KCl, respectively (determined dilution factor of vesicles is 1.2). Addition of valinomycin immediately induces a negative potential in K^+-loaded vesicles in Na^+-buffer and a positive one in Na^+-loaded vesicles in K^+-buffer (*14*).

Vesicle Aggregation Induced by Pep-1. Vesicle aggregation was monitored by optical density (OD) at 436 nm as described elsewhere (*15*). Briefly 6.88 μM pep-1 was added to a LUV suspension; additional lipid suspension aliquots were added after signal stabilization. LUVs of POPC or of different molar ratios of POPC and POPG (4:1 and 1:1) were prepared. Initial and final lipidic concentrations used in the assays were 25 and 106 or 106 and 222 μM, respectively. The pep-1 concentration effect was tested with POPC/POPG (1:1) vesicles; 0.54, 1.45, 3.40, and 6.88 μM pep-1 concentrations were used. Fluorescence microscopy studies were carried out with POPC vesicles doped with 1% of N-Rh-PE, a 510−550 nm excitation filter, and a 590 nm band-pass filter. The final lipidic and pep-1 concentrations used were 0.1 and 1.45 or 6.88 μM, respectively.

LUV Fusion and Anionic Lipid Segregation Induced by Pep-1. Fusion was tracked using the Forstër resonance energy transfer (FRET)-based methodology described before by others (*16*−*18*). Briefly, vesicles doped with both 1% N-NBD-PE (donor) and 1% N-Rh-PE (acceptor) and unlabeled vesicles were mixed; after that, 0.54, 1.45, or 6.88 μM pep-1 was added. If fusion between unlabeled vesicles and donor/acceptor-labeled vesicles occurs, the average distance between donors and acceptors increases, that is, FRET efficiency decreases. POPC, POPC/POPG (4:1), and POPC/POPG (1:1) were used (final lipid concentrations of 50 and 100 μM). Fluorescence intensity was followed with λ_{exc} = 463 nm (NBD absorption) and λ_{em} = 590 nm (Rh emission). Control experiments were carried out in all cases. Fluorescence quenching of Rh by pep-1 was evaluated by adding pep-1 (0−6.88 μM) to 1% N-Rh-PE doped vesicles to establish the minimal fluorescence intensity decrease expected (i.e., corresponding to fusion absence). The other end of the fusion scale (100%) was calculated by adding excess TX-100 surfactant (0.2% v/v) to the vesicle suspension. Fusion extent was calculated by linear interpolation between these limits.

Pep-1-induced anionic lipid segregation was also followed by FRET between NBD and Rh. Fluorescence emission intensity of Rh B dependence on pep-1 concentration (0−6.88 μM) was monitored in LUVs of POPC and POPC/POPG (4:1) containing 1% C6-NBD-PG and 1% N-Rh-PE. Final lipidic concentrations of 0.05, 0.1, and 1 mM were used. Control assays were carried out with C6-NBD-PC (zwiterionic) instead of C6-NBD-PG.

Pore Formation and Phospholipid Flip-Flop. Co^{2+} is an aqueous quencher of NBD fluorescence (*19*, *20*) and is accessible to N-NBD-PE and C6-NBD-PC inserted in vesicles (*20*). Pore formation was tested as described previously by others (*20*). Briefly vesicle suspensions of POPC, POPC/POPG (4:1), DPPC, and DPPC/DPPS (4:1) containing 1% N-NBD-PE were prepared in the absence and presence of 20 mM $CoCl_2$. In vesicles prepared without Co^{2+}, the quencher was added after LUV formation to guarantee that Co^{2+} is accessible only to NBD present in the external layer. No significant shrinkage was detected by turbidimetry in agreement with the small effect expected for vesicles upon osmolality variation due to 20 mM Co^{2+} (in/out osmolality ratio = 0.83; see Figure 1 in ref *21*). NBD fluorophores derivatized in the polar group of phospholipids inhibit flip-flop (*17*, *22*) given the hydrophilic nature of the probe and its localization (*17*). The same methodology was used to study flip-flop, but LUVs were doped with 1% C6-NBD-PC or 1% C6-NBD-PG. Phospholipids derivatized in short acyl chains can undergo flip-flop (*23*−*25*). Flip-flop was studied in POPC and DPPC LUVs. Fluorescence emission intensity (λ_{exc} = 460 nm and λ_{em} = 531 nm; excitation wavelength is optimized for best NBD/Co^{2+} absorbance

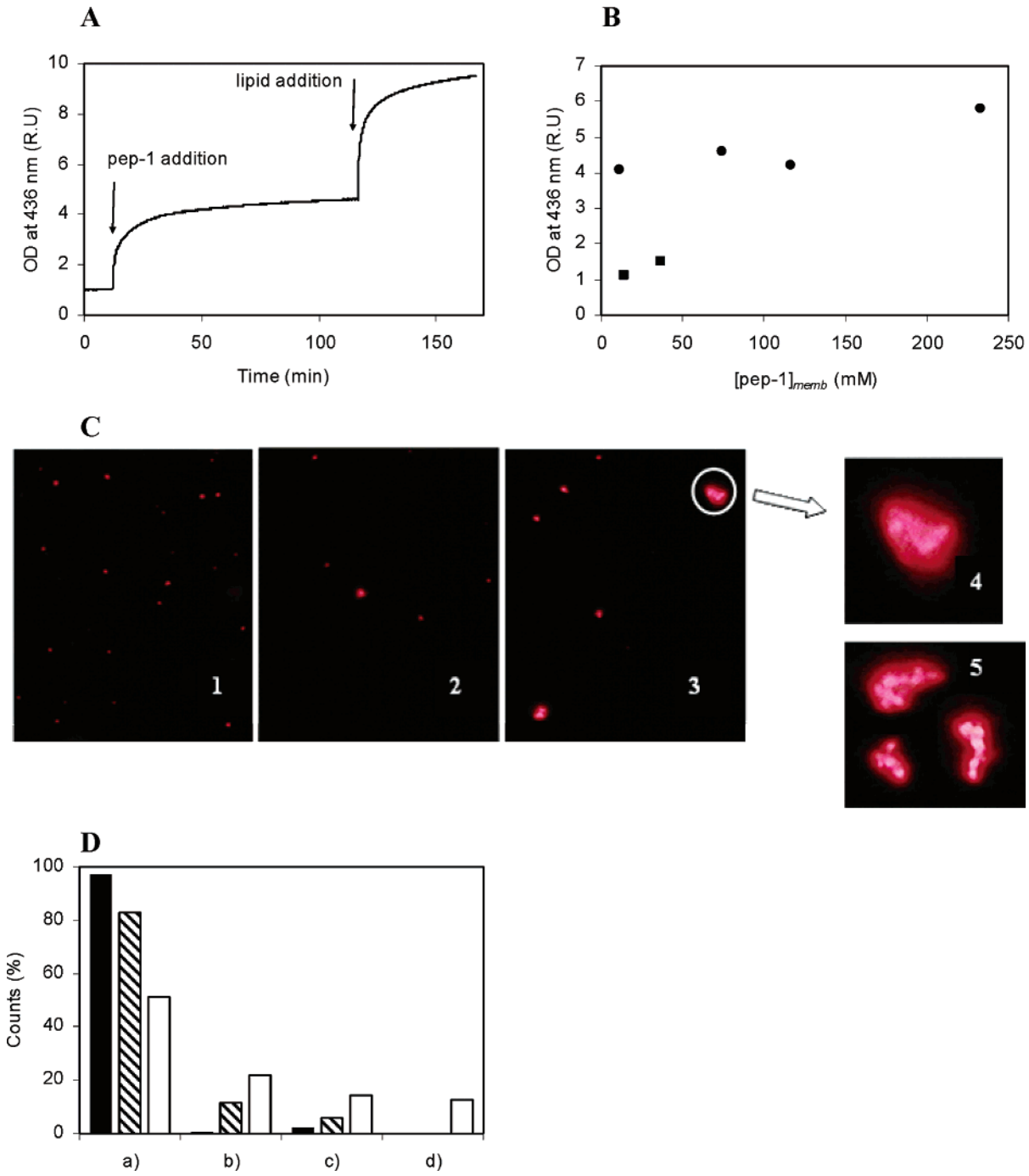

FIGURE 1: Vesicle aggregation induced by pep-1. Panel A shows the time course of the optical density (OD) at 436 nm showing aggregation of POPC/POPG (4:1) LUVs. After signal stabilization, 6.88 μM pep-1 was added to the 25 μM lipidic suspension in 10 mM HEPES buffer, pH 7.4, containing 150 mM NaCl. Peptide addition induced vesicle aggregation. Further addition of vesicle suspension to a 106 μM lipidic concentration induces more vesicle aggregation. Panel B shows the dependence of the normalized OD at 436 nm of a 25 μM lipidic suspension of POPC, POPC/POPG (4:1), and POPC/POPG (1:1) LUVs on pep-1 effective concentration in the membrane (eq 10 in ref *26*) below (■) and above (●) critical concentration for aggregate organization (3.4 ± 1.7 μM; ref *11*) (see Table 1). Panel C shows micrographs of POPC LUVs doped with 1% N-Rh-PE obtained by fluorescence microscopy with a 510−550 nm excitation filter and a 1000× amplification (1) in the absence and in the presence of (2) 1.45 and (3) 6.88 μM pep-1. In micrograph 3, less and larger bright units (aggregated vesicles) are presented. Fusion of subunits occurs as seen in amplifications 4 and 5 (6.88 μM pep-1). It is possible to identify different LUV subunits that constitute the aggregates. Panel D shows the percentage of bright units in preparations of POPC LUVs doped with 1% N-Rh-PE observed by fluorescence microscopy with a 510−550 nm excitation filter (filled columns refer to control, hatched to 1.45 μM pep-1 addition, and unfilled to 6.88 μM pep-1): (a) bright units where only one LUV could be noticed, (b) aggregates where fusion already occurred, and (c,d) aggregates formed by 2−3 and 4 or more units, respectively.

ratios) was recorded before and after 1.45 and 6.88 μM (final concentrations) pep-1 addition. Control assays without Co^{2+} were performed. The lipid concentration used was 100 μM. The data values were corrected for the inner filter effect (*19*).

Pore formation was also evaluated in LUVs loaded with 30 μM rhodamine B. Buffer containing the desired Rh B concentration was added to the lipidic film prior to MLV formation; after the extrusion step, the vesicle suspension

was eluted through a 10 mL Econo-Pac 10DG column (Bio-Gel P-6DG gel with 6 kDa molecular weight exclusion) packed with buffer (without Rh B) to remove nonencapsulated Rh B. Encapsulated Rh B fluorescence intensity was recorded ($\lambda_{exc} = 554$ nm and $\lambda_{em} = 576$ nm) prior to and after addition of 1.45 and 6.88 μM peptide.

Translocation Assays. Vesicles doped with 1% N-Rh-PE (100 μM total lipid concentration) were used to evaluate fluorescence emission quenching of Rh by pep-1. The Rh emission fluorescence intensity was monitored at $\lambda_{exc} = 570$ nm and $\lambda_{em} = 590$ nm.

To study translocation in absence of transmembrane potential, POPC and POPC/POPG (4:1) MLVs were prepared in the absence and presence of 1.45 or 6.88 μM peptide. Vesicles prepared directly in pep-1 suspensions are controls because in this case pep-1 is accessible to Rh fluorophores present in all lamellae. In the other experiments, pep-1 was added to MLVs prepared in absence of pep-1 to a final concentration of 1.45 or 6.88 μM. The assays were repeated in the presence of 1 mM phosphine. Usage of MLVs enables a gradual effect in case translocation occurs.

Transbilayer potentials were created in POPC, POPC/POPG (4:1), and POPC/POPG (1:1) vesicles (see Preparation of Lipid Vesicles). Pep-1 was added to vesicles to a final concentration of 6.88 μM. After the fluorescence signal was constant, valinomycin was added to vesicles at a $1:10^4$ molar ratio (mol/mol lipid; *14*; from ethanolic solution; final ethanol concentration 0.2%). Controls without valinomicin (i.e., in the absence of a transmembrane potential) were also prepared. Pore formation (in POPC/POPG (4:1) LUVs) and flip-flop (of C6-NBD-PC and C6-NBD-PG in POPC LUVs) were also evaluated (see methodology in previous section) in the presence of negative transmembrane potential. Valinomycin was added after addition of 6.88 μM pep-1.

RESULTS AND DISCUSSION

Pep-1 Induced Vesicle Aggregation. Vesicle aggregation is dependent on three main forces (*15*): electrostatic repulsion, van der Waals attraction, and hydration. Multivalent cations may alter the charge density at the vesicles surfaces, as well as dehydrate the lipid polar groups, and therefore eventually lead to aggregation of vesicles. Pep-1 is a multivalent cation that anchors at the lipidic membrane interface (*11*): this prompted us to study the effect of pep-1 on aggregation of vesicles. When the peptide is added to LUVs of POPC/POPG 4:1 (molar), the optical density of the solution slowly increases (Figure 1A) until a plateau is reached ~100 min later. Further addition of lipids results in a second increase in optical density (Figure 1A), that is, lipid addition does not revert the vesicle aggregation, at variance to penetratin-induced aggregation (*15*). Table 1 presents data that account for the effect of anionic lipids, total lipidic concentration, and peptide concentration on vesicle aggregation ability. Effective concentration of the peptide at the lipidic environment was calculated in all cases to enable direct comparisons (see ref *11* and eq 10 in ref *26*). The main experimental evidences from Table 1 are as follows: (1) Anionic lipids favor aggregation, although the effect is relatively weak (Figure 1B). (2) Addition of lipids to increase the total lipid concentration also leads to further aggregation (Figure 1A); when penetratin is used, the opposite effect is observed (*15*), suggesting that pep-1 and penetratin do not coincide in their mode of action at molecular level. (3) The optical density obtained upon peptide addition when the initial lipidic concentration is 106 μM is different from the one obtained when initial lipidic concentration is 25 μM and is increased to 106 μM after peptide addition. The final dimension of vesicle aggregates does not depend on the lipidic concentration, only. Stepwise addition of lipid results in bigger aggregates (in terms of light scattering intensity, the effect of volume change superimposes to the simultaneous process of scattering particle concentration decrease). One possible explanation is the ability of pep-1 to add isolated vesicles to previously formed aggregates but inability to cluster large previously formed aggregates. Stepwise addition of vesicles enlarges previously formed aggregates rather than create new small aggregates. (4) Pep-1 organization in the aqueous environment (i.e., 1.45 vs 6.88 μM in Table 1) influences vesicle aggregation (Figure 1B).

Table 1: Vesicle Aggregation Induced by Pep-1

lipid	[lipid] (μM)[a] initial/final	X_L[b] initial/final	$[pep\text{-}1]_T$ (μM)	$[pep\text{-}1]_{memb}$ (mM)[c] initial/final	OD[d] peptide/lípid
POPC	25/106	0.03/0.12	6.88	11.3/10.3	4.1/7.9
		0.12/0.23	6.88	10.3/9.08	4.8/8.2
POPC/POPG (4:1)	25/106	0.17/0.47	6.88	74.1/69.5	4.6/9.5
	106/222	0.47/0.65	6.88	69.5/63.8	4.4/6.9
POPC/POPG (1:1)	25/106	0.49/0.80	0.54	13.8/5.35	1.1/1.2
			1.45	37.1/14.7	1.5/1.9
		0.65/0.89	3.44	117/37.7	4.2/6.0
			6.88	233/75.4	5.8/8.8

[a] Before peptide addition, lipid concentration was 25 or 106 μM; after more lipid was added, the final concentration became 106 or 222 μM, respectively. [b] The molar fraction of peptide inserted in lipid (X_L) was determined by eq 3 in ref *34* using partition coefficients for pep-1 (*11*). [c] Pep-1 concentration in lipidic bilayer by application of eq 10 in ref *26*. [d] Optical density (OD) at 436 nm (normalized to [pep-1] = 0) of POPC and POPC/POPG vesicles (prepared in 10 mM HEPES, pH 7.4, buffer containing 150 mM NaCl) after peptide, first number, and more lipid addition, second number (see Figure 1B).

Fluorescence microscopy studies using POPC vesicles doped with N-Rh-PE confirm aggregation (Figure 1C). Pep-1 addition results in less and bigger bright units relative to the control in the micrographs. At higher pep-1 concentration, aggregation of smaller units is noticeable with a magnification of 1000× (Figure 1C,D). Because turbidity is proportional to the squared volume of scattering entities, a small fraction of big aggregates may lead to high optical density values.

Peptide-induced vesicle aggregation implies a severe reduction in vesicle stability due to a decrease in electrostatic repulsion and interference with the hydration layer. This second factor seems dominant since POPC vesicle aggregation is quite significant and similar to the one obtained with POPC/POPG (i.e., anionic vesicles).

Pep-1 Induced Vesicle Fusion. Vesicle fusion implies that (1) the inner content of two or more vesicles is mixed and (2) lipids from previously separated bilayers coexist in the same bilayer after fusion (*27*). Fusion may result from a variety of stimuli (*27*). Pep-1 induced lipidic vesicle fusion seems plausible because vesicle aggregation (see previous section) creates propitious conditions (*28*). Moreover, pep-1 is amphipathic, which is a common characteristic among fusiogenic peptides (*18*).

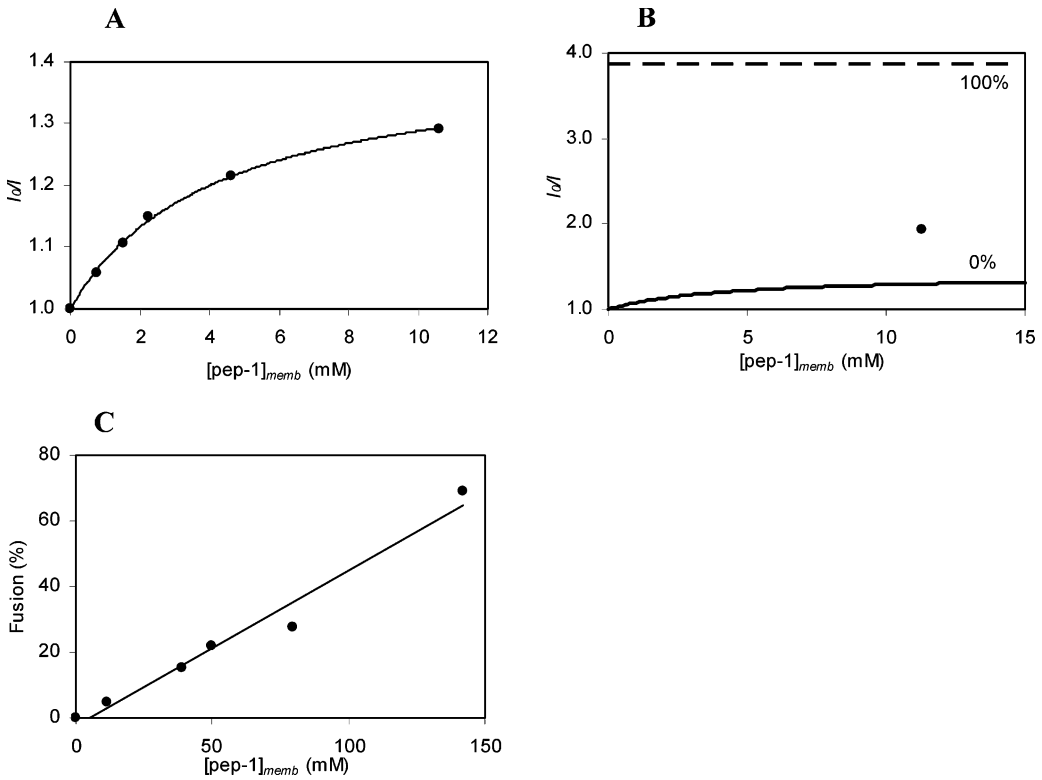

FIGURE 2: Vesicle fusion induced by pep-1. Fusion assays were monitored by FRET between NBD (donor) and rhodamine B (acceptor) (λ_{ex} = 463 nm; λ_{em} = 590 nm; sensitized emission of acceptor). Vesicle suspensions doped with 1% N-NBD-PE and 1% N-Rh-PE were prepared in 10 mM HEPES, pH 7.4, buffer containing 150 mM NaCl. Panel A shows a Stern−Volmer plot of the fluorescence emission quenching of 100 μM POPC LUVs doped with 1% N-Rh-PE (λ_{em} = 570 nm; λ_{ex} = 590 nm) by pep-1 (the effective pep-1 concentration in membrane is considered; eq 10 in ref *26*). The Lehrer equation (see eq 11 in ref *26*) was fitted to the data (solid line). Panel B shows the relative fusion scale of 50 μM POPC/POPG (4:1) LUVs; 0% fusion (full line) is obtained by the Stern−Volmer plot of the Rh B quenching by pep-1 (Figure 2A), and 100% fusion (dashed line) is the fluorescence emission of vesicle suspensions in excess TX-100. Effective peptide membrane concentration in the membrane is used for the sake of comparison with other LUV compositions since the extent of peptide partition is dependent on the anionic lipid composition. The filled circle refers to the fluorescence intensity obtained by addition of 6.88 μM total concentration of pep-1. Fusion percentage (22.1%) was calculated from linear interpolation. Panel C shows the fusion percentage in POPC and POPC/POPG LUVs. All data were obtained in the presence of 6.88 μM pep-1 total concentration; however, effective concentration in membranes vary (see Table 2). Fusion extension and effective concentration in membranes are linearly correlated.

Table 2: Vesicle Fusion Induced by Addition of Pep-1

lipid	[lipid] (mM)	$[\text{pep-1}]_T$[a] (μM)	$[\text{pep-1}]_{memb}$[b] (mM)	I_0/I[c] (0% fusion)	I_0/I[d] (100% fusion)	I_0/I (assay)	fusion (%)[e]
POPC	0.05	6.88	11.3 ± 3.9	1.30 ± 0.61	4.35 ± 0.07	1.45 ± 0.02	4.9 ± 0.07
POPC/POPG (4:1)	0.05	6.88	49.8 ± 39.8	1.38 ± 1.27	3.87 ± 0.09	1.93 ± 0.004	22.1 ± 0.05
	0.1	6.88	39.0 ± 31.2	1.37 ± 1.27	3.15 ± 0.05	1.64 ± 0.02	15.2 ± 0.18
POPC/POPG (1:1)	0.05	0.54	9.3 ± 6.7	1.28 ± 1.08	3.98 ± 0.09	1.21 ± 0.02	0
		1.45	24.9 ± 17.9	1.35 ± 1.13	3.98 ± 0.09	1.38 ± 0.02	1.1 ± 0.02
		6.88	141.7 ± 85.6	1.40 ± 1.02	3.98 ± 0.09	3.18 ± 0.07	69.0 ± 1.5
	0.1	6.88	79.3 ± 47.9	1.38 ± 1.00	3.28 ± 0.05	1.90 ± 0.03	27.4 ± 0.43

[a] Refers to total pep-1 concentration in bulk solution. [b] Refers to effective peptide in lipidic matrix. [c] Refers to pep-1 quenching fluorescence of rhodamine B. [d] Refers to the addition of Triton X-100. [e] The vesicle fusion percentage of different lipidic mixtures (POPC, POPC/POPG (4:1) and POPC/POPG (1:1)) in 10 mM HEPES, pH 7.4, buffer containing 150 mM NaCl was determined as illustrated in Figure 2B. Results are presented along with standard errors.

The FRET-based methodology described elsewhere (*16*−*18*) to study vesicle fusion was adapted to account for the N-Rh-PE fluorescence quenching by pep-1 (Figure 2A). The Rh fluorescence intensity depends on the exact effective pep-1 concentration in the membrane environment, $[\text{pep-1}]_{memb}$ (see eq 10 in ref *26*, reported as $[Q]_L$), even in the absence of fusion because N-Rh-PE fluorescence is quenched by pep-1. This fluorescence emission intensity corresponding to 0% fusion is calculated from the Stern−Volmer formalism (Figure 2A,B). In excess TX-100, donor/acceptor mean interdistance becomes much bigger than the Förster radius, R_0, minimizing the fluorescence intensity (100% of the fusion scale). Figure 2B illustrates the data analysis procedure. NBD quenching by TX-100 (*18*) is not relevant for our purpose.

The results obtained using different lipid concentrations, lipidic charge densities, and pep-1 concentration are presented in Table 2. Fusion is only significant when $[\text{pep-1}] = 6.88\ \mu$M, which is also true for aggregation. Anionic lipids may not have a direct role in fusion. POPG interference with fusion may result from enhanced partition into the membrane (*11*). When fusion percentage is plotted as a function of $[\text{pep-1}]_{memb}$ for systems having different anionic charge densities and lipid concentrations (Figure 2C), one single homogeneous data set is obtained. Thus, $[\text{pep-1}]_{memb}$ seems to be

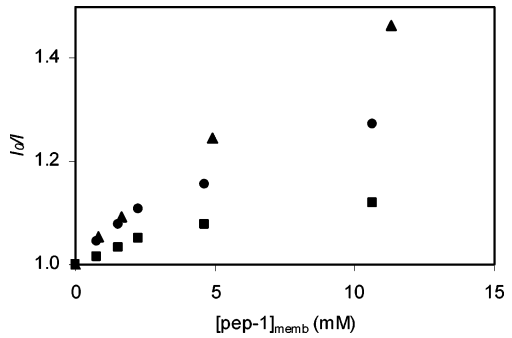

FIGURE 3: Anionic lipid segregation induced by pep-1. The assays were followed by FRET between NBD (donor) and rhodamine (acceptor) (λ_{ex} = 463 nm; λ_{em} = 590 nm; sensitized emission of acceptor). The POPC vesicle suspension was prepared with 1% N-Rh-PE and 1% C6-NBD-PG (or C6-NBD-PC in the control assay, ■) in 10 mM HEPES, pH 7.4, buffer containing 150 mM NaCl. The total lipidic concentrations used were 50 (▲) and 100 μM (●). A more pronounced decrease of Rh B fluorescence intensity relative to the control assay means a greater distance between donor and acceptor, that is, segregation of anionic lipids near the partition local of pep-1 in vesicles.

the key regulator issue in vesicle fusion. Pep-1 organization in the aqueous environment is another important factor (no fusion detected in 1.45 μM pep-1 solution). Fusiogenic activity is usually associated with α-helix conformation in membranes (*18*). This suggests that pep-1 may adopt α-helix conformation at 6.88 μM in the presence of lipidic bilayers. However, direct evidence from CD spectroscopy, for instance, is prevented due to the typical low sensitivity of these techniques.

Pep-1 Induced Anionic Lipid Segregation. Some cell-penetrating peptides such as penetratin are believed to have their biochemical mode of action dependent on the interaction with anionic lipids (*29*). Electrostatic interaction is essential for lipidic bilayer structure perturbation afterward. To test the hypothesis that perturbation results from peptide-induced anionic lipid lateral redistribution in the membranes, we used NBD-labeled PG (anionic) and Rh-labeled PE (zwitterionic) in POPC vesicles and carried out FRET experiments. Anionic lipid segregation results in a decrease in FRET efficiency in the presence of peptide. Control experiments were carried out using NBD-labeled PC instead of PG (the quenching of Rh B by the peptide is accounted for in the control). Figure 3 shows that pep-1-induced anionic lipid segregation occurs to an extent that depends both on the lipidic and on the peptide concentrations. Variations in FRET efficiency are not detected when 20% (molar) POPG is present in the vesicles (results not shown), as expected due to the "dilution" of anionic lipidic probes in excess anionic lipids.

Pore Formation in the Absence of Transmembrane Potential. Some membrane-interacting peptides, such as mellitin, possess unspecific lytic ability (*30*, *31*). Mellitin resembles pep-1 for the presence of a proline residue in its sequence (*27*) among other reasons. These similarities prompted us to test pep-1-induced pore formation across lipidic membranes. Co^{2+} is an aqueous quencher of NBD fluorophores (*19*, *20*) and was used to quench N-NBD-PE inserted in LUVs in the presence and absence of pep-1 (a method based on previously published ones (*19*)). In the absence of pep-1, Co^{2+} is expected to leave 50% of the N-NBD-PE fluorophores accessible if added to a LUV suspension after vesicles are formed and all the fluorophores

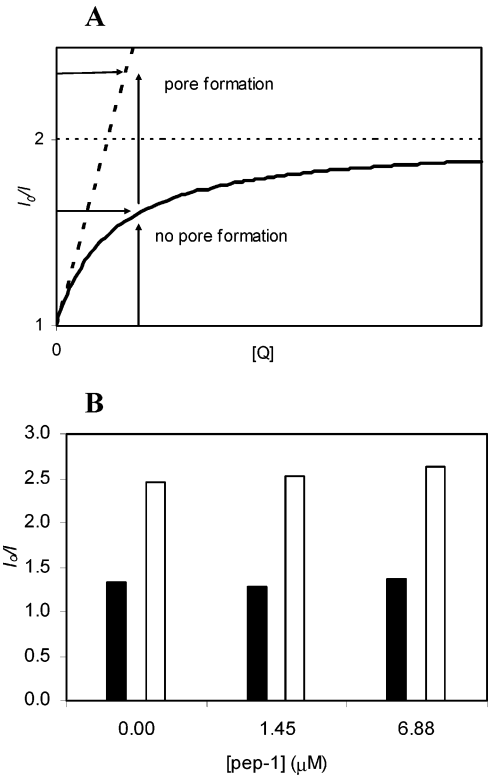

FIGURE 4: Vesicle pore formation induced by pep-1. Co^{2+} quenching of fluorescence emission of LUVs doped with 1% N-NBD-PE (λ_{em} = 460 nm; λ_{ex} =531 nm) was performed to test for pep-1-induced pore formation in vesicles. Vesicles with 20 mM Co^{2+} accessible to both layers and vesicles with 20 mM quencher accessible just to external layer have been produced in a 10 mM HEPES, pH 7.4, buffer containing 150 mM NaCl. In panel A, the hyperbole-like curve (full line) simulated with the Lehrer equation with f_B = 50% (see eq 11 in ref *26*) indicates the NBD fluorescence quenching of the latter vesicles in the case of no pore formation. If the addition of pep-1 leads to a more pronounced quenching (dashed line), near linearity (the limit where the quencher is accessible to all NBD fluorophores) pores are formed. At a given quencher concentration, I_0/I, can be used to account for pore formation. Panel B shows the ratio of NBD intensity of 100 μM POPC LUVs in the absence of quencher and in the presence of 20 mM Co^{2+} for the vesicles with Co^{2+} accessible to both layer (white columns) and accessible only to the outer layer (black columns). Comparing the results with control, it is possible to conclude that there is no pore formation in the presence of 1.45 or 6.88 μM pep-1.

if it is added before vesicles are formed. In the case that pores or other lytic perturbations are formed by the peptide, Co^{2+} first present only outside lipidic vesicles is able to penetrate vesicles and reach all the fluorophores, that is, the quenching extent is dependent on lytic perturbations of the membrane induced by pep-1 (Figure 4A). Results presented in Figure 4B show that no lytic action occurs in POPC vesicles because peptide presence does not change NBD quenching by Co^{2+}. Similar results were obtained with POPC/POPG (4:1) vesicles (results not shown). These results were confirmed in LUVs with encapsulated Rh B (dissolved in buffer). The addition of pep-1 does not induce a significant quenching of Rh B fluorescence emission (data not shown), revealing that peptide is inaccessible to vesicle lumen and that there is no ion leakage.

Asymmetric Lipidic Flip-Flop in the Absence of Transmembrane Potential. Flip-flop refers to the lipidic exchange between outer and inner layers (*23*) and may be promoted by peptide insertion in membranes (*23*, *24*). Peptides perturb

membranes causing defects at the interfacial packing that allow passage of the polar lipidic heads through the aliphatic region of membranes (*24*). The same methodology used before for pore formation assays was used to test for asymmetric lipidic flip-flop, except that C6-NBD-PC and C6-NBD-PG were used instead of N-NBD-PE. The latter probe does not translocate across membranes due to the bulky NBD residue at its polar head (*17*). Results (not shown) do not present evidence of asymmetric flip-flop of lipids in any of the lipidic systems tested (POPC and DPPC with and without anionic lipids). In case that flip-flop occurs at all, it is bidirectional and occurs at the same rate in the inner/outer and opposite direction.

Peptide Translocation across Lipidic Bilayers. The biochemical activity of pep-1 is related to its ability to translocate across lipidic membranes. Translocation assay methodologies were based on the peptide quencher properties relative to Rh B (Figure 2A). We prepared MLVs with peptide solutions from the start (samples A) or buffer without peptide. In the latter samples, peptide was added after vesicle formation (samples B) to the final peptide concentration used in samples A. In the case that translocation occurs, fluorescence intensity in samples B decreases with time until the fluorescence intensity of samples A is reached. No translocation was detected in POPC and POPC/POPG (4:1) vesicles both in the absence (Figure 5A) and presence of phosphine (results not shown).

Previous studies have shown that translocation of peptidic sequences across a synthetic bilayer is largely stimulated in the presence of a transmembrane potential (*14*, *32*, *33*). In a recently published work, Terrone et al. (*32*) showed that penetratin translocation in LUVs is mediated by transbilayer potential in a manner dependent on vesicle composition. The effect of transbilayer potential in pep-1 translocation was evaluated in POPC, POPC/POPG (4:1), and POPC/POPG (1:1) doped with N-Rh-PE. After peptide addition to LUVs, a significant fluorescence quenching of Rh B emission fluorescence was recorded in studied lipidic systems ($I_0/I \approx 2$, which is an expected value because in these conditions pep-1 is accessible only to Rh B in the external layer). If translocation occurs in the presence of a transbilayer potential, an increase of Rh emission fluorescence quenching is expected (pep-1 is accessible to Rh in the internal layer). The presence of valinomycin-induced negative transbilayer potential (maximum transbilayer potential about 120 mV (*32*, *33*), stable for 10 min (*14*)) in K^+-loaded vesicles in Na^+-buffer causes a significant translocation of pep-1 in POPC/POPG (4:1) and POPC/POPG (1:1) (Figure 5B) on the second time scale. In POPC, the translocation occurs to a minor extent. The rapid translocation is in agreement with in vivo studies (*8*) that show translocation of the peptide across cell membranes on the minute time scale. The effect of a positive transbilayer potential was tested in POPC/POPG (4:1) vesicles. The addition of valinomycin to Na^+-loaded vesicles in K^+-buffer does not alter the fluorescence emission quenching of Rh B by pep-1. This result shows that a positive transbilayer potential does not lead to translocation. Similar results were obtained with vesicles dispersed in buffer containing 150 mM KCl (K^+ in and out) and with vesicles prepared in buffer with 150 mM NaCl (Na^+ in and out).

Figure 5C, which represents a Stern−Volmer-like plot, shows that translocation is dependent on the effective

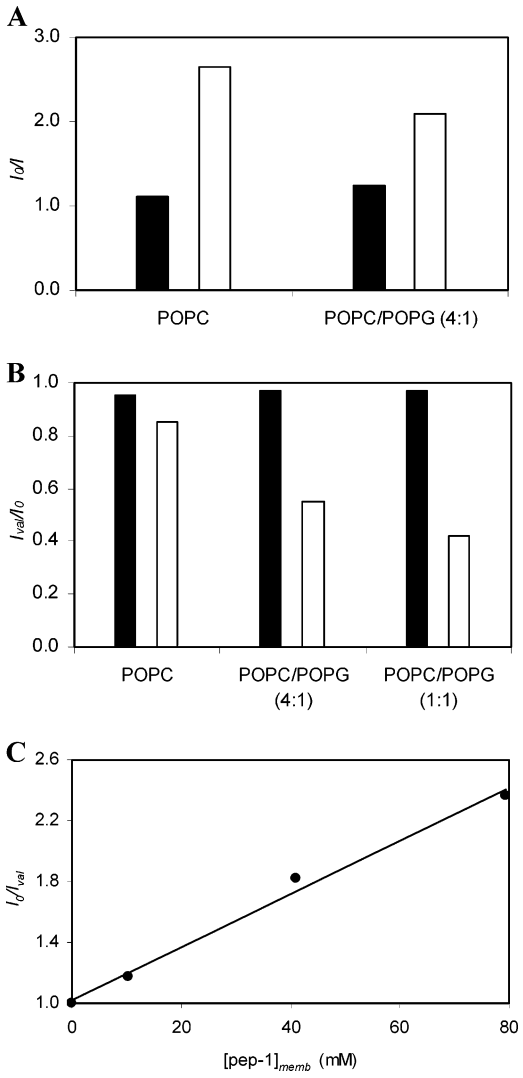

FIGURE 5: Pep-1 translocation across lipidic bilayer. Translocation assays were followed by fluorescence quenching of rhodamine B ($\lambda_{ex} = 570$ nm; $\lambda_{em} = 590$ nm) by pep-1 in 100 μM vesicles doped with 1% N-Rh-PE. In panel A, POPC and POPC/POPG (4:1) MLVs (10 mM HEPES, pH 7.4, buffer containing 150 mM NaCl) were used. The results are presented in terms of intensity ratio without and with 6.88 μM pep-1 added at the moment of the vesicle preparation (white columns) and after the vesicle preparation (black columns). In case translocation exists, the same fluorescence intensity is expected for both columns. No peptide translocation was detected. Panel B shows translocation of pep-1 in the presence of transmembrane potential in POPC, POPC/POPG (4:1), and POPC/POPG (1:1) LUVs (loaded with 10 mM HEPES pH 7.4 buffer containing 150 mM KCl and dispersed in buffer containing 150 mM NaCl). Rhodamine B fluorescence emission was recorded, and a decrease to approximately half of the initial value was detected after 6.88 μM pep-1 addition (pep-1 accessible to N-Rh-PE in external layer). The Rh B fluorescence intensity ratio after (I_{val}) and before (I_0) addition of valinomycin ($1{:}10^4$ mol/mol lipid) is represented for the three lipidic systems in the presence (white columns) and absence (black columns) of 6.88 μM pep-1. A decrease in I_{val}/I_0 upon valinomycin addition (negative transmembrane potential) indicates that pep-1 is accessible to N-Rh-PE in the inner layer and translocation across bilayer occurs. An enhanced effect is visible with an increase in anionic lipid. Panel C shows a Stern−Volmer-like plot, which represents I_0/I_{val} (see panel B) dependence on effective pep-1 concentration in membrane (see eq 10 in ref *26*). Translocation extension is dependent on effective pep-1 concentration in membrane (increases with peptide concentration in membrane).

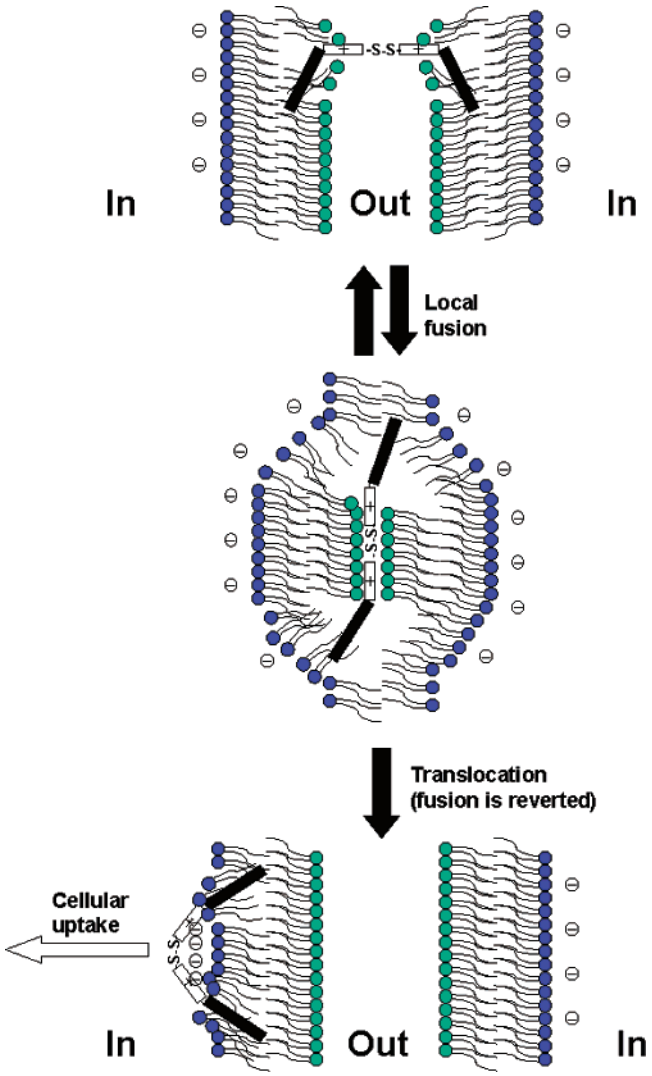

FIGURE 6: Putative pep-1 translocation mechanism across lipidic bilayer. This scheme outlines a possible mechanism for pep-1 translocation. The peptide has the ability of inserting in the bilayer outer interface and causes local and transient fusion of membranes (experimental results show clustering of vesicles without collapse and no lytic lesions). Transiently fused biological membranes (negatively charged inner face) bring the cationic sequences of the peptide closer to the anionic inner leaflet of the membranes. In this situation, electrostatic attraction is strong enough to move pep-1 to one of the inner leaflets of the membranes and segregate anionic lipids. The inverted micelle-like structure originated from fusion is then reverted. The partition equilibrium in the cell inner lipidic hemilayer is shifted toward the nonlipidic environment due to the reduction of pep-1 dimers (*11*) and cellular uptake. The role of partition equilibria in the regulation of pep-1 action across lipidic bilayers is addressed in ref *11*.

concentration of peptide in membrane ($[\text{pep-1}]_{\text{memb}}$). The results show that the translocation driving force is the negative membrane potential across bilayer and affinity of peptide to membrane determines the extent of translocation.

In the presence of negative transmembrane potential, no significant drop in NBD fluorescence was detected, when valinomycin was added (after 6.88 μM pep-1 addition) to POPC/POPG (4:1) LUVs doped with N-NBD-PE or to POPC vesicles doped with C6-NBD-PC or C6-NBD-PG (Co^{2+} accessible to the external layer of the vesicles in both cases). Fluorescence intensities with the quencher accessible to internal and external layers were used as a positive control. No pore formation or significant phospholipid flip-flop occurs during peptide translocation (data not shown).

CONCLUSION

Pep-1 is effective in inducing vesicle aggregation and lipidic fusion. Aggregation takes place by vesicle clustering, but lipidic exchange among vesicles is possible. The process is dependent both on anionic lipid content and on peptide concentration. Segregation of anionic lipids in the presence of peptide is detected. Despite all these effects, no evidence was found for lytic action or ion leakage. Translocation occurs only in vesicles with a negative membrane potential and is enhanced by the presence of anionic lipids, probably by electrostatic attraction of the peptide to anionic bilayers.

Taking our work as a whole, one concludes that the main driving force for peptide translocation is a charge gradient across membrane (negative inside). In biological membranes, the transmembrane potential caused by charge asymmetry between outer and inner leaflets created by anionic lipids in the inner layer is probably responsible for translocation. Moreover, pep-1 is a strong perturber of lipid membrane organization (Figure 6), which is probably a key role of its action because the energetic cost of solvation layer removal (mandatory for crossing an unperturbed membrane) would be prohibitive. Bilayer perturbation renders electrostatic attraction dominant over solvation effects. As proposed schematically in Figure 6, fusion is probably the main cause of close range electrostatic attraction between positively charged peptide and negatively charged lipids in the cell membrane inner leaflets. Transient inverted micelle-like structures may be formed, leading to translocation. An active role of membrane aggregation in translocation was very recently proposed for the cell-penetrating peptide penetratin (*32*).

ACKNOWLEDGMENT

We thank Dr. Fernando Antunes and Nuno M. V. Pedroso for helping with fluorescence microscopy and Dr. M. Prieto and Dr. Cláudio Soares for valuable critical discussions.

REFERENCES

1. Wadia, J. S., Becker-Hapak, M., and Dowdy, S. F. (2002) Protein transport, in *Cell-penetrating peptides, processes and applications* (Langel, Ü., ed) pp 365−375, CRC Press Pharmacology & Toxicology Series, CRC Press, New York.
2. Bogoyevitch, M. A., Kendrick, T. S., Dominic, C. H., and Barr, R. K. (2002) Taking the cell by stealth or storm? Protein transduction domain (PTDs) as versatile vectors for delivey, *DNA Cell Biol. 21*, 879−894.
3. Bonetta, P. (2002) Getting protein into cells, *Scientist 17*, 38−40.
4. Eguchi, A., Akuta, T., Okuyama, H., Senda, T., Yokoi, H., Inokuchi, H., Fujita, S., Hayakama, T., Takeda, K., Hasegawa, M., and Nakanisshi, M. (2001) Protein transduction domain of HIV-1 Tat protein promotes efficient delivery of DNA into mammalian cells, *J. Biol. Chem. 247*, 27205−27210.
5. Richard, J. P., Melikov, K., Vives, E., Ramos, C., Verbeure, B., Gait, M. J., Chernomordik, L. V., and Lebleu, B. (2003) Cell-penetrating peptides, a reevaluation of the mechanism of cellular uptake, *J. Biol. Chem. 278*, 585−590.
6. Schwarze, S. R., Hruska, K. A., and Dowdy, S. F. (2000) Protein transduction: unrestricted delivery into all cells? *Trends Cell Biol. 10*, 290−295.
7. Chaloin, L., Mau, N. V., Divita, G., and Heitz, F. (2002) Interactions of cell-penetrating peptides with membranes, in *Cell-penetrating peptides, processes and applications* (Langel, Ü., ed)

pp 23−51, CRC Press Pharmacology & Toxicology Series, CRC Press, New York.
8. Morris, M. C., Depollier, J., Mery, J., Heitz, F., and Divita, G. (2001) A peptide carrier for the delivery of bilogically active proteins into mammalian cells, *Nat. Biotechnol. 19*, 1143−1147.
9. Chariot, simple efficient protein delivery system. http://www.activemotif.com/products/cell/chariot (accessed July 2003).
10. Morris, C. M., Chalion, L., Heitz, F., and Divita, G. (2002) Signal sequence-based cell-penetrating peptides and their application for gene delivery, in *Cell-penetrating peptides, processes and applications* (Langel, Ü., ed) pp 93−113, CRC Press Pharmacology & Toxicology Series, CRC Press, New York.
11. Henriques, S., and Castanho, M. (2004) Environmental factors that affect the cell penetrating peptide pep-1 action across lipidic membranes, *Chem.Phys.Chem.* submitted for publication.
12. Wieprecht, T., Beyermann, M., and Seeling, J. (2002) Thermodynamics of the coil-α-helix transition of amphipathic peptides in membrane in a membrane environment; the role of vesicle curvature, *Biophys. Chem. 96*, 191−201.
13. Mayer, L. D., Hope, M. J., and Cullis, P. R. (1986) Vesicles of variable sizes produced by a rapid extrusion procedure, *Biochim. Biophys. Acta 858*, 161−168.
14. van Dalen, A., Killian, A., and de Kruijff, B. (1999) $\Delta\psi$ stimulates membrane translocation of the C-terminal part of a signal sequence, *J. Biol. Chem. 274*, 19913−19918.
15. Persson, D., Thorén, P. E. G., and Nordén, B. (2001) Penetratin-induced aggregation and subsequent dissociation of negatively charged phospholipid vesicles, *FEBS Lett. 505*, 307−312.
16. Haugland, R. P. (2002) *Handbook of Fluorescent Probes and Research Products*, 9th ed., Molecular Probes, New York.
17. Maier, O., Oberle, V., and Hoekstra, D. (2002) Fluorescent lipid probes: some properties and applications (a review), *Chem. Phys. Lipids 116*, 3−18.
18. Pécheur, E.-I., Martin, I., Ruysschaert, J.-M., Bienvenüe, A., and Hoekstra, D. (1998) Membrane fusion induced by 11-mer anionic and cationic peptides: a structure−function study, *Biochemistry 37*, 2361−2371.
19. Caputo, G. A., and London, E. (2003) Using a novel dual fluorescence quenching assay for measurement of tryptophan depth within lipid bilayes to determine hydrophobic α-helx location within membranes, *Biochemistry 42*, 3265−3274.
20. Chattopadhyay, A., and London, E. (1988) Spectroscopic and ionization of N-(7-nitrobenz-2-oxa-1,3-diazol-4-yl)-labeled lipid in model membranes, *Biochim. Biophys. Acta 938*, 24−34.
21. Pencer, J., White, G. F., and Hallet, F. R. (2001) Osmotically induced shape changes of large unilamellar vesicles measured by dynamic light scattering, *Biophys. J. 81*, 2716−2728.
22. Wimley, W. C., and White, S. H. (2000) Determining the membrane topology of peptides by fluorescence quenching, *Biochemistry 39*, 161−170.
23. Kol, M. A., Laak A. N. C. van, Rijkers, D. T. S., Killian, J. A., Kroon, A. I. P. M. de, and Kruijff, B. de (2003) Phospholipid flop induced by transmembrane peptides in model membranes is modulated by lipid composition, *Biochemistry 42*, 231−237.
24. John, K., Schreiber, S., Kubelt, J., Herrmann, A., and Müller, P. (2002) Transbilayer movement of phospholipids at the main phase transition of lipid membranes: implications for rapid flip-flop in biological membranes, *Biophys. J. 83*, 3315−3323.
25. Marx, U., Lassmann, G., Holzhütter, H.-G., Wüstner, D., Müller, P., Höhlig, A., Kubelt J., and Herrmann A. (2000) Rapid flip-flop of phospholipids in endoplasmic reticulum membranes studied by a stopped-flow approach, *Biophys. J. 78*, 2628−2640.
26. Santos, N. C., Prieto, M., and Castanho, M. A R. B. (1998) Interaction of the major epitope region of HIV protein gp41 with membrane model systems. A fluorescence study, *Biochemistry 37*, 8674−8682.
27. Basañez, G. (2002) Membrane fusion: the process and its energy suppliers, *Cell. Mol. Life Sci. 59*, 1478−1490.
28. Nieva, J. L., and Nir, S. (2000) Interactions of peptides with liposomes: pore formation and fusion, *Prog. Lipid Res. 39*, 181−206.
29. Dupont, E., Joliot, A., and Prochiantz, A., (2002) Penetratins, in *Cell-penetrating peptides, processes and applications*, (Langel, Ü., ed) pp 23−51, CRC Press Pharmacology & Toxicology Series, CRC Press, New York.
30. Matsuzaki, K., Yoneyama, S., and Miyajima, K. (1997) Pore formation and translocation of melitin, *Biophys. J. 73*, 831−838.
31. Papo, N., and Shai, Y. (2003) Exploring peptide membrane interaction using surface plasmon resonance: differentiation between pore formation versus membrane disruption by lytic peptides, *Biochemistry 42*, 458−466.
32. Terrone, D., Sang, S. L. W., Roudaia, L., and Silvius, J. R. (2003) Penetratin and related cell-penetrating cationic peptides can translocate across lipid bilayers in the presence of a transbilayer potential, *Biochemistry 42*, 13787−13799.
33. Maduke, M., and Roise, D. (1993) Import of a mitochondrial presenquence into protein-free phospholipid vesicles, *Science 260*, 364−367.
34. Santos, N. C., Prieto, M., and Castanho, M. A R. B. (2003) Quantifying molecular partition into model systems of biomembranes: an emphasis on optical spectroscopic methods, *Biochim. Biophys. Acta 1612*, 123−135.

BI036325K